Dynamics of Poly(styrenesulfonate) Sodium Salt in Aqueous Solution

Rongjuan Cong, Elena Temyanko, Paul S. Russo,* Nadia Edwin, and Rao M. Uppu†

Chemistry Department and Macromolecular Studies Group, Louisiana State University, Baton Rouge, Louisiana 70803

Received June 5, 2005; Revised Manuscript Received November 8, 2005

ABSTRACT: The diffusion of poly(styrenesulfonate) sodium salt (NaPSS) was investigated using dialysis dynamic light scattering (DLS) and dialysis fluorescence photobleaching recovery (FPR). Never-dried or "virgin" NaPSS was synthesized directly from 4-styrenesulfonic sodium salt to achieve 100% sulfonation. Upon reducing the ionic strength directly in the DLS cell by dialysis, a clean sample developed clearly distinct fast and slow modes that were first identified as an extraordinary phase in low-salt solutions of poly-L-lysine by Lin, Lee, and Schurr [*Biopolymers* **1978**, *17*, 1041]. This result complements published polyelectrolyte investigations in a high-dielectric constant organic solvent, and also studies where the degree of ionization was tuned, which confirms that hydrophobic patches along the polymer chain are not required for the extraordinary behavior. The fast mode dominated even at low ionic strength, with scattering amplitude exceeding 70% of the total. For the virgin NaPSS sample in the dialysis cell, there is no convincing evidence of a slow mode at high salt (≥200 mM NaCl). The appearance of distinct slow and fast modes proved reversible upon removing and adding salt by dialysis, without any other perturbation save restoration of the concentration by dialysis centrifugation. This suggests that the behavior represents a thermodynamically equilibrated state. Dialysis FPR measurements of aqueous solutions of a commercial NaPSS that was labeled with fluoresceinamine (LNaPSS) showed no obvious long-range ordering. A reversible decrease in the optical tracer self-diffusion coefficient of LNaPSS as salt is dialyzed out of the solution is instead attributed to chain expansion. Comparison of FPR and DLS on a mixed LNaPSS/NaPSS sample suggests that the residence time of a chain in temporal aggregates [Schmitz et al. *Biopolymers* **1984**, *23*, 1637] that are thought to be responsible for the DLS slow mode is shorter than the FPR time scale.

Introduction

The behavior of polyelectrolytes at low ionic strength has attracted much attention in the quarter century since the dynamic light scattering (DLS) observations by Lin, Lee, and Schurr[1] of a sudden transition as NaBr was removed from solutions of poly-L-lysine at finite concentration, c_p. The lasting impression of that study is its Figure 1, which showed apparent diffusion coefficient, D_{app}, plotted against salt concentration, c_s. In that figure, D_{app} rose as the salt was reduced and then precipitously dropped below a particular value of c_s that was higher for larger polymer concentrations. The effect was so sudden and dramatic that the authors associated it with the appearance of a new, extraordinary "phase" associated with changes in scattering intensity, not only dynamics. As the authors were aware,[2] low intensities are easily understood from a thermodynamic treatment of scattering,[3] which shows that intensity is inversely proportional to the osmotic modulus $(\partial\Pi/\partial c_p)_T$ where Π is the osmotic pressure. Compressing dissolved polyelectrolytes requires great amounts of osmotic pressure to overcome the mutual repulsion of highly charged chains, especially at low salt where charges are not screened. The spontaneous occurrence of fluctuations, and associated scattering, is correspondingly low.

The small fluctuations that do occur in an osmotically stiff system relax quickly, which is oddly reminiscent of the rapid decay of forced oscillations in stiff, elastic solids. A thermodynamic explanation is easy: the mutual diffusion coefficient sensed by DLS is proportional to osmotic modulus,[4] $D_m \sim (\partial\Pi/\partial c_p)_T$; however, a molecular interpretation proves elusive. The theory of Lin, Lee, and Schurr[2] has been applied with mixed results,[5−7] prompting statements like this one:[7] "It is generally accepted that the fast mode reflects the diffusive properties of single macroions or at least large segments of single macroions." The writers are not claiming that whole chains or even segments of them separately translate the distance scale of DLS (several thousand angstroms) at rates comparable to those of solvents and small ions. DLS measures the collective motions of many chains to relax local refractive index inhomogeneities. This knowledge does not help the present authors, at least, visualize how such very fast apparent diffusion coefficients arise on the DLS distance scale. If the motions responsible are longitudinal (in the sense of being parallel to the scattering vector or to the Fourier component of segment density sensed by the light scattering experiment), they must be coupled over very long distances. It is possible for transverse (in the sense of being perpendicular to the scattering vector) motions to have consequences over long distances, even though the only displacements may be over short distances, but these modes are not ordinarily associated with DLS. One's imagination is challenged to understand the fast mode on a molecular basis. In the words of Sedlak (italics ours),[8] "Nevertheless, eigenmodes (*and associated decay rates*) in general can be identified with simple types of motions (that can be easily visualized) only in very special cases."

The slow decay mode is not very well understood, either. Lin, Lee, and Schurr noted that the autocorrelation functions remained bimodal or perhaps multimodal below the proposed ordinary−extraordinary transition. Even though it was difficult to study multimode decays with the linear correlators of that era, evidence was soon available to suggest that more than one decay process was simultaneously present.[6,9,10] Early studies by methods other than scattering failed to confirm any unusual behavior at the ordinary−extraordinary transition.[11−13] Schmitz and Ramsay[10] applied oscillating electrical fields while measur-

* To whom correspondence should be addressed: e-mail chruss@lsu.edu.
† Present address: Department of Environmental Toxicology and The Health Research Center, Southern University, Baton Rouge, LA 70813.

10.1021/ma051171x CCC: $33.50
Published on Web 12/16/2005

Table 1. Characterization of Poly(styrenesulfonate) Sodium Salt

sample	source	M_w	M_w/M_n	data source
virgin NaPSS	synthesized for this work	586 000	1.2	this work
NaPSS-70K	SP^2 Inc.	70 000	1.4	ref 48
LNaPSS-167K	fractionated from labeled NaPSS-70K	167 000	1.3	this work
LNaPSS-70K	labeled from NaPSS-70K SP^2 Inc.	70 000	1.4	ref 48

ing the spectral broadening of scattered light, in an attempt to identify the role of ions in the scattering from chains and temporal aggregates. Scattering mode amplitudes associated with the slow decay process have been plotted against scattering angle to obtain apparent sizes in the 600−1000 Å range.[14,15] Small-angle neutron scattering data also tie the slow mode to the formation of multimacroion domains in about this same size range.[16] The internal structure and dynamics of the macroions are beginning to be illuminated by neutron spin echo experiments.[17] Papers by Sehgal and Seery[18] and Sedlak[8] are recommended for additional perspective on the controversial[8,14,16,18−35] slow mode topic; it will be seen that some studies find that the slow and fast modes coexist over a wide range of concentrations. Nevertheless, the transition criterion identified by Drifford and Dalbiez[6] remains a convenient landmark. For monovalent salts, this concentration is $c_{DD} = c_p(a/l_B)$ where a is the charge separation along the backbone and l_B is the Bjerrum length, at which separation of two like charges generate a potential energy equal to the molecular thermal energy, kT, where k is Boltzmann's constant and T the kelvin temperature. For aqueous NaPSS, $a \approx 2.5$ Å and $l_B \approx 7$ Å.

This paper is devoted to expanding the phenomenology of the slow mode and to the development of better tools for the study of polyelectrolytes in general. One concern is the purity of the polyelectrolyte itself. Commercially produced NaPSS, the most commonly chosen model polymer, is made by sulfonating polystyrene. Even under harsh conditions, the process is imperfect.[36,37] Residual hydrophobic patches along the chains may group together, leading to aggregation. This has been addressed by experiments in solvents even more polar than water[18] and/or using weak polyelectrolytes,[7,16,19,38,39] whose hydrophobic character can be altered by adjusting the charge on titratable groups. A second concern is that freeze-drying may result in more aggregates.[21,22] A third issue is filtering, which might remove the aggregates or domains, even though it has also been implicated in the formation of slow modes through contact with the hydrophobic filter bodies.[21,22,29,40] A fourth problem is contact with trace amounts of hydrophobic substances. Studies of aqueous solutions of poly(ethylene oxide), an uncharged macromolecule, suggest that trace hydrophobic impurities acquired during synthesis or processing may be responsible for slow modes.[41] The same could happen for charged molecules, especially those with hydrophobic patches. One source of slow modes that does not worry us in this study is very high concentration, which leads to slow intensity fluctuations related to viscoelastic behavior.[42−45]

To address these issues, we synthesize a unique "virgin" NaPSS sample directly from 4-styrenesulfonic sodium salt in an aqueous medium to give 100% degree of sulfonation and therefore no hydrophobic defects. No drying procedures are involved, and the material does not come into contact with hydrophobic impurities. The behavior of virgin NaPSS is investigated with dialysis DLS, in which the solution is contained in a DLS cell fitted with a dialysis membrane. This simplifies studies of the effects of salt, including reversibility. Changes can be brought about by dialyzing against the desired salt solutions in the scattering cell; no extra filtration steps are required. As optical tracer diffusion methods provide a valuable companion to scattering-based investigations of strongly interacting systems, including polyelectrolyte solutions,[11,18,34,46,47] we also label a commercial NaPSS with fluoresceinamine and directly compare the transport properties of labeled NaPSS (LNaPSS) with DLS and FPR. Unlike the virgin NaPSS for the dialysis DLS study, this material may have hydrophobic patches due to incomplete sulfonation. Some of the measurements are done in an FPR dialysis cell, with the same advantages already noted for dialysis DLS. The critical assumption is that attachment of a very small amount of dye does not substantially change the properties of a polymer chain, which seems to be the case.[48,49] The number of comparable studies is limited[11,18,34] and does not yet include aqueous LNaPSS.

Experimental Section

Materials. 4-Styrenesulfonic sodium salt, 2,2′-azobis(isobutyronitrile) (AIBN), and fluoresceinamine isomer I were bought from Sigma-Aldrich. Dimethyl sulfoxide (DMSO) and methanol were bought from Fisher Scientific. All the chemicals were used without further purification. Water was supplied by a five-stage Barnstead Nanopure system that includes a spiral-wound, 5 nm ultrafilter. Polymer characterization data appear in Table 1.

Synthesis. Virgin poly(styrenesulfonate) sodium salt (NaPSS) with 100% degree of sulfonation was synthesized with free radical polymerization of 4-styrenesulfonic sodium salt. 5.0 g of 4-styrenesulfonic sodium salt, 10 mg of AIBN, 20 g of water, and 20 g of methanol were added into a 100 mL round-bottomed flask. The mixture was purged with argon for 30 min at room temperature. The polymerization was started by gradually increasing temperature to 75 °C and terminated after 20 h by leaking air into the system. The raw product was concentrated by purging N_2 filtered through a 0.2 μm PTFE filter to eliminate most of the methanol, leaving water as the major solvent.

Purification of Virgin NaPSS Solution. The raw product was further purified by ultracentrifugation and resuspension in Nanopure water in an Ultrafree-4 centrifugal filter unit with molecular weight cutoff of 10 000 (Millipore Inc.). The design of these devices is such that the solution above the ultrafilter membrane "floor" never goes dry in a fixed angle rotor. One of the advantages of centrifugation and resuspension was to reduce polydispersity, as low molecular weight NaPSS chains and the residual reactants passed through the centrifugal filter, thus resulting in a relatively narrow distributed virgin NaPSS sample. The purity of virgin NaPSS was confirmed with ^{1}H NMR, which showed the correct ratio of aromatic:alkyl resonances. Details appear in the Supporting Information.

Determination NaPSS Concentration by UV Absorbance. Thermogravimetric analysis (TA Instruments Universal V2.6D) showed that NaPSS is hygroscopic, with two water molecules per styrenesulfonate repeating unit, as reported by Prabhu et al.[50] The extinction coefficient ϵ was found to be 1.837 mL/mg at 262 nm and 48.28 mL/mg at 220 nm, which is close to the results from other researchers.[51] Care was taken to remove residual Na_2SO_4 in the standard NaPSS sample from SP^2 Inc. Additional details appear in the Supporting Information.

Molecular Weight Characterization. The molecular weight characterization of virgin NaPSS was obtained by GPC/multiple-angle laser light scattering (GPC/MALLS) using a Waters 401 differential refractive index detector and a Wyatt DSP light scattering detector (operating at 16 different angles, wavelength 632.8 nm). The specific refractive index increment, dn/dc, was taken as 0.198 mL/g.[51] The GPC column set consisted of Polymer Labs

(Amherst, MA) PL Aquagel-OH mixed 8 μm (one mixed column plus one 50 Å column). A 50 mM NaCl solution was used as the mobile phase at a flow rate of 1.0 mL/min. The injection volume was 100 μL. The mean and standard deviation of the weight-averaged molecular weight (M_w) were estimated from three measurements.

DLS. After a painstaking procedure (Supporting Information) to clarify the virgin NaPSS sample, dialysis DLS was conducted directly on the sample in a Centricon YM-3 centrifugal concentrator, which has a clear plastic upper half for scattering observation. Discarded was the lower half, which normally collects fluid when the device is used as intended for concentrating samples. The bottom of the upper half of the YM-3 is made of dialysis membrane with a nominal 3000 molecular weight cutoff (MWCO), which is sufficient to retain the polymers used. The dialysis membrane permits direct exchange of salt or change of pH without the need to refilter the sample. These alterations can be made directly in the scattering device by choosing for its index matching fluid the aqueous solution desired. Centering of the cell is not critical, as the beam suffers only small displacements (and not deflections) on traversing the container. Use of an index-matching fluid that does not have the same refractive index as the cell is not much of a problem; mismatch always exists between aqueous samples and the inner surfaces of glass containers anyway. During transitions to lower ionic strength, the sample swells, which must be reversed by removing it from the bath, reattaching the collecting lower half of the cell, and centrifuging. This might seem to open the door to centrifugal force and associated hydrostatic pressure as a new potential source of aggregates/domains, but the effects described below can be observed without reconcentrating the diluted samples after dialysis to lower ionic strength. The samples were maintained at 25 °C and measured at scattering angles of 30°−95° using laser wavelengths λ_0 of 514.5, 532, or 632.8 nm depending on the strength of the scattering signal and presence of dye molecules. At low ionic strength, the low scattered intensity necessitates long acquisition times, increasing the chance for dust artifacts. The detailed procedure to accomplish this task reliably is reported in the Supporting Information.

FPR and Dialysis FPR. Commercial NaPSS was labeled in a two-step reaction: chlorination of the sulfonate group followed by the attachment of fluoresceinamine.[48] Chlorination can be achieved with a $PCl_3/POCl_3$ mixture[52] or pure $POCl_3$.[48] A higher efficiency of chlorination was reported with the $PCl_3/POCl_3$ mixture.[48] Pure $POCl_3$ was chosen for the labeling because a very low efficiency of chlorination leads to the desired light labeling. A broad-distribution NaPSS-70K sample was used as the starting material for labeling. Higher molecular weight LNaPSS-167K was obtained by the fractionation of LNaPSS-70K (see Supporting Information). The molecular weight was analyzed with the GPC/MALLS apparatus generally following conditions reported earlier.[49] For most of the FPR experiments, single-exponential analysis proved adequate, reflecting the relatively narrow dispersion of the LNaPSS samples. For the dialysis FPR, a third-order polynomial fit, resembling cumulant analysis in DLS,[53] was also used to make a conclusion regarding the effect of salt on the size polydispersity. FPR samples were prepared 48 h before measurement and loaded into rectangular capillary cells (Vitrocom, Mountain Lakes, NJ). Other FPR details were previously reported.[54,55]

Dialysis FPR took advantage of a newly constructed cell, in which the sample was sandwiched between a semipermeable membrane and a standard microscope cover glass. Details will be provided when discussing its performance in the Results and Discussion section. Briefly, the dialysis exchange fluid was kept in a 500 mL bottle immersed in the same water bath for temperature equilibration. After a sample was loaded, a 10 min period was waited to allow for thermal equilibration. The initial self-diffusion coefficient was measured at one value of the instrumental spatial frequency, K, with three repeat runs. During measurements of the effect of added salt on self-diffusion of LNaPSS, the required amount of NaCl was added to the dialysis fluid and 15 min was allowed for equilibration. The temperature was controlled by circulating water with a water bath (NESLAB RTE-111).

Results and Discussion

Dialysis Dynamic Light Scattering. Once a dust-free sample is loaded into the dialysis cell, the effect of added salt and its reversibility can be tested easily by changing the salt concentration in the external dialysis solution. Thus, dialysis DLS eliminates tedious refiltering procedures, the associated chance of introducing contaminants, and the possibility of breaking any mechanically weak structures. The lowest possible ionic strength ($\sim 5 \times 10^{-6}$ M for samples exposed to the atmosphere) can be achieved easily. In the external dialysis vat, Nanopure water that had been passed through a 0.1 μm Millipore Millex VV filter (to remove particulates in an intermediate vessel—Nanopure water itself is almost perfectly free of dust) was used in order to reduce stray light. During some studies, the pH and salt conditions were varied by changing the contents of this vat directly. Usually, it proved a more efficient use of instrument time to remove the cell and perform exchanges against a solution in a separate vessel.

One disadvantage of dialysis DLS in an open cell is dramatic dilution upon lowering the ionic strength. The Centricon YM-3 cells described above are designed for concentration, so restoring the original concentration was trivial. Another disadvantage, this time specific to the simple cells we chose, is mediocre optical performance. The laser beam must not be permitted to strike scratches on the cells. Optical performance was evaluated by measuring the scattered intensity of Nanopure water in a dialysis cell from 45° to 110°. The intensity corrected for scattering angle and normalized by the reading at $\theta = 90°$ (i.e., $I \sin(\theta)/I_{90}$) was 1.025 ± 0.023. This is good for a mass-produced plastic cell in a water index matching vat. Temperature was controlled by placing a separate tube into the dialysis/index matching vat through which circulated water from a temperature-regulated bath. During measurements, contact between the dialysis/index matching bath and the cell was normally interrupted by blowing a bubble underneath the membrane. The circulation of thermostat water was stopped just before DLS measurement to avoid possible vibration; as the measurements were always near room temperature, this resulted in negligible errors.

In one experiment, virgin NaPSS in 700 mM NaCl was directly added into an extensively cleaned (see Supporting Information) Centricon filter unit. A starting solution of 700 mM NaCl was chosen because shrinkage of the NaPSS chains allows the use of a small filter, such as a 0.02 μm Whatman Anotop. It is expected that NaPSS molecules, collapsed by the added salt, pass through while dust particles >0.02 μm are retained to the extent possible using filters, which are always imperfect devices. After passing through the cascade of filters (Supporting Information) while still at elevated salt, the cleanliness of the sample was confirmed. Dust was not observed visually at 100× magnification at a scattering angle of 30°, and DLS experiments of 3000 s duration at 45° revealed no intensity spikes.

Figure 1 shows two intensity autocorrelation functions measured under identical optical conditions. The sample is the same 2.6 g/L virgin NaPSS solution in the same cell. Two different salt concentrations were achieved by dialysis, starting from 700 mM NaCl (where the scattering profile was dominated by a single mode, not shown). After dialysis against 3 mM NaN_3, a distinctly biexponential correlation function appeared, and the zero-time intercept, $g^{(2)}(0)$, was depressed to just 1.27. At 3 mM NaN_3, this sample lies just below the Drifford−

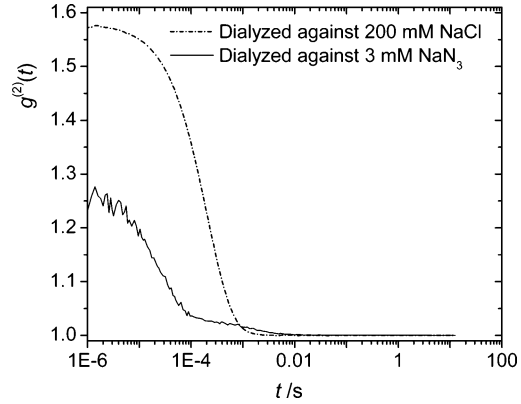

Figure 1. Correlation functions in dialysis light scattering cell under identical optical conditions ($\lambda_0 = 514.5$ nm, $\theta = 45°$) with and without salt, as indicated.

Dalbiez concentration (~4.5 mM for $c_p = 2.6$ mg/mL). When the sample was dialyzed back against 200 mM NaCl, the behavior returned to normal, with only one clearly evident decay mode (the possibility of additional detail is discussed at length in the Supporting Information). The intercept increased to 1.57, almost the value for a strong scatterer measured with the instrumental parameters in effect (1.63).

The reduction in the intercept $g^{(2)}(0)$ at the lower ionic strength shown in Figure 1 implies that the excess intensity from the polymer is not large compared to the intensity scattered by the solvent. The system has become osmotically "stiff"; the fluctuations in polymer concentration, which cause light scattering, are small in amplitude at the spatial frequencies being probed. The above-the-baseline intercept of an ideal homodyne DLS correlation function is described[56] by a coherence parameter, $0 < f < 1$, such that $g^{(2)}(t) = 1 + f|g^{(1)}(t)|^2$, where $g^{(1)}(t)$ is the first-order, electric field correlation function. The two correlation functions in Figure 1 exhibit $f = 0.27$ (low salt) and 0.57 (high salt). The realizable coherence is reduced when the solvent accounts for an appreciable portion of the scattered light because correlators cannot track the rapid fluctuations due to solvent motion. Ignoring photomultiplier dark count (as appropriate for these experiments), we may write $f = f_{max}[A_p/(A_p + A_{solv})]^2$, where f_{max} is the coherence parameter observed for a strong scatterer with the same optical settings. The symbols A_p and A_{solv} stand for the polymer and solvent signals, respectively. Using $f_{max} = 0.63$ and $f = 0.27$, one finds that the scattered intensity during the low-salt measurement shown in Figure 1 was 1.9 times that of pure water. The slow decay process in Figure 1 represents 27% of the $g^{(1)}(t)$ signal (not to be confused with the coincidental $f = 0.27$ value). Thus, the intensity associated with the slow mode is about $0.27 \times 1.9 = 0.51$ times the scattering strength of pure water. Some investigators[18,31] have used benzene as an intensity reference; it scatters about 14 times more strongly than water.[57] The scattering strength of the slow mode evident in Figure 1 under conditions of low salt is ~3.5% that of benzene.

The apparent cleanliness of the sample deteriorated slightly after dialyzing against 3 mM NaN_3. The practice of acquiring multiple short runs allows us to inspect each one for any indication of dust before being included in the average, thus eliminating the effect of large dust particles. The slower decay mode evident in Figure 1 survived this scrutiny. Virgin NaPSS genuinely exhibits a biexponential decay at low ionic strength.

The effect of added salt on virgin NaPPS solutions is reversible. This suggests that the structures underlying the slow mode originate from thermodynamic interactions among the

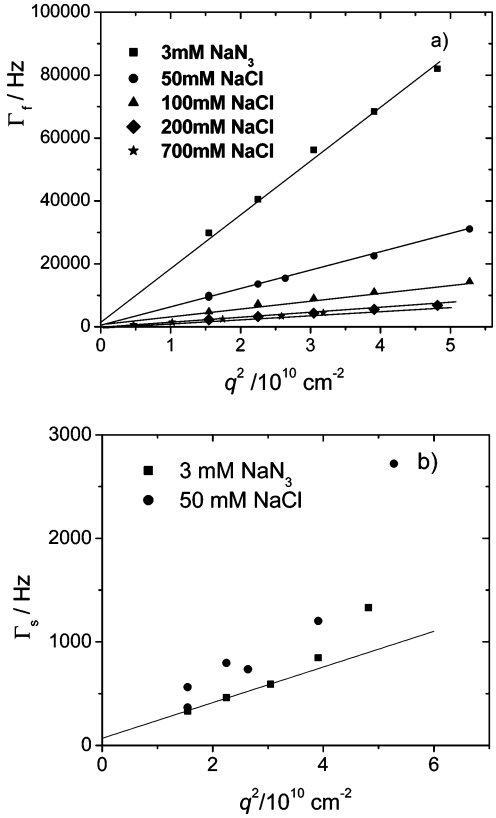

Figure 2. Correlation function decay rates as a function of squared scattering vector for the salt concentrations indicated: (a) fast mode; (b) slow mode.

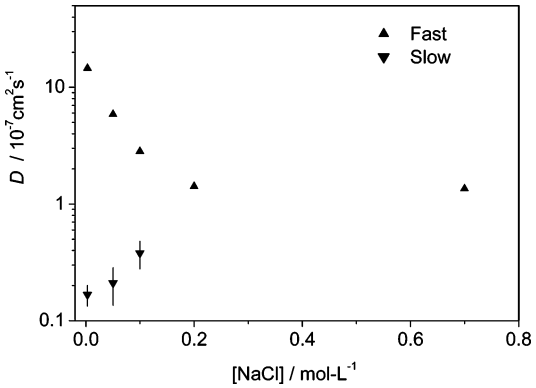

Figure 3. Apparent slow- and fast-mode diffusion coefficients for 2.6 mg/mL "virgin" NaPSS.

expanded NaPSS chains, although a recent study on the mechanical properties of multimacroion domains suggested that such changes are partially irreversible.[28] It has also been suggested that filtering itself can initiate the domains.[29] In the dialysis cell, the slow mode structures appear without such provocation.

The combined slow and fast mode behavior for virgin NaPSS at various salt concentrations is shown in Figures 2 and 3. Using CONTIN Laplace inversion software,[58,59] biexponential behavior became distinct when the salt concentration decreased to less than 200 mM. Two closely spaced, almost equally strong modes can be fit to the data at 200 mM NaCl or even at 700 mM NaCl by using a simpler, two-exponential nonlinear least-squares analysis; however, it is argued in the Supporting Information that this is a consequence of the intrinsic, though modest, polydispersity of the virgin NaPSS sample, not temporal aggregates. At low salt (<200 mM NaCl) the faster of the two

decay modes is surely diffusive because the relation $\Gamma_f = D_f q^2$ holds (Figure 2a).

It is harder to ascertain the diffusive behavior of the weaker and slower mode, but at 50 mM NaCl it appears to follow $\Gamma_s = D_s q^2$ at lower values of q (Figure 2b). The upward curvature at higher q, also observed at 50 mM NaCl, suggests structures that are large, polydisperse, physically extended or some combination of these. D_f was calculated from $D_f = \Gamma_f/q^2$, and the apparent D_s values were estimated similarly, despite the poorer correlation. As shown in Figure 3, the apparent diffusion coefficients of the two modes differ by orders of magnitude (this is unlike the two-exponential fits to an essentially unimodal correlation function above 200 mM salt; those two decay modes differ only by a factor of about 3, as discussed in the Supporting Information). The fast mode gets faster, and the slow mode slower, as salt is reduced. For reference, $c_{DD} \sim 4.5$ mM at the polymer concentration pertaining to Figure 3.

In some ways, these results are consistent with the findings of so many others. The observation of two diffusive modes for virgin NaPSS at low salt confirms conclusively that the widely observed behavior does not require hydrophobic segments on the chain, aggregates formed during drying, trace impurities acquired during isolation or filtering, etc. On the other hand, there seem to be some unusual results.

The fast mode dominates at low ionic strength in our studies, comprising over 70% of the signal. The benzene equivalent scattering level of the slow mode, 3.5% according to the above analysis, can also be computed by comparison to a benzene reference in the manner described by Sedlak.[31] That method is superior at high salt, where the coherence parameter, f, is not significantly depressed. In this lab, toluene is used as an internal reference, but the conversion to a benzene reference is straightforward.[57] The upshot of these calculations is that the slow mode increases in strength with c_s, reaching about 23% of the benzene scattering level at 100 mM before falling to invisibility by 200 mM NaCl, to within the uncertainty of the experiment (as discussed in the Supporting Information). Although the slow mode amplitudes here are much smaller than generally observed, the rise−fall trend is familiar.[18,31] Differences in sulfonation, handling, equilibration time, and concentration are the most likely explanations for the variation between this work and previous studies. Parameter selection during data analysis is considered in the Supporting Information; it is easy to generate artifacts at the level of several percent of total signal when using CONTIN, and one must carefully watch the amplitude error bars to guard against this, but the consistent trends in other studies argue against CONTIN abuse as an explanation for stronger slow modes. Even the optical settings or design of a DLS spectrometer might affect the results. A conventional DLS instrument (one using apertures and pinholes to obtain high spatial coherence) sees a very small volume, typically compensating for that with a powerful laser. Some newer instruments use single mode or nearly single mode fibers to select larger volumes without the penalty of spatial incoherence, permitting the use of weaker and less expensive lasers well mated to efficient detectors. In the former kind of instrument, used in most studies to date, care must be taken to include enough scatterers, thereby avoiding number fluctuations. For samples containing a sparse population of large particles that one desires to measure, the conventional instrument will struggle to make an accurate reading. Long acquisition times will ensure that the large particles are observed, but never simultaneously in large enough numbers to avoid contributions from ill-behaved number fluctuations[56] with a characteristic time that depends on the detected volume (and hence scattering angle). The single mode fiber type of instrument may give a better representation of the larger particles—at the risk of increased interference from dust. The conventional instrument can be set to see larger volumes, incurring a reduction of coherent signal over baseline. No study of slow mode amplitude with optical settings has appeared. Finally, virgin NaPSS solutions show a certain degree of inhomogeneity at low ionic strength. For some repeat runs, an extra mode, even slower and possibly weaker in amplitude than the one discussed above, was detected. Higher quality data, requiring much longer acquisition times, would be necessary to elucidate details about this mode. In summary, there are many possible reasons for variations in the mode strengths observed by different groups.

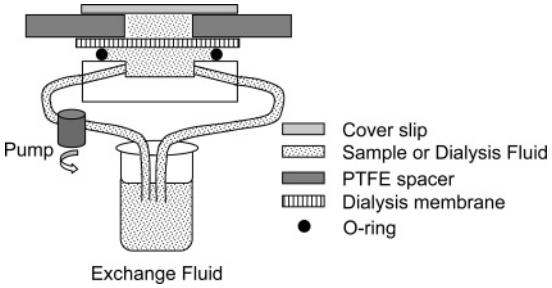

Figure 4. Schematic of the dialysis FPR cell.

Dialysis FPR. As noted by earlier workers,[11] the problems associated with acquiring and interpreting DLS data on polyelectrolyte solutions provide strong motivation to try other methods, especially FPR[11,18] and DOSY.[60] As it did seem that the in-situ dialysis just described made DLS easier, an effort was mounted to bring the same convenience to the already-more-convenient (despite the labeling steps) FPR method. Thus, an in-situ dialysis implementation of FPR was developed to study the effect of salt on the self-diffusion coefficient of fluoresceinimine-tagged NaPSS. Commercially available NaPSS, instead of virgin NaPSS, was used as the starting material for dye attachment. A promising method for preparing labeled, virgin NaPSS with essentially perfect sulfonation was developed,[49] but not in time for these studies. Multimacroion domains have been widely reported in DLS studies of commercially available NaPSS in the literature.

The dialysis FPR cell was constructed as shown in Figure 4. The 200 μL sample is sandwiched between a microscope cover glass, which is bonded after 24 h of annealing at room temperature, under modest pressure, to an etched Teflon sheet with a thickness of 0.3 mm (Small Parts, Inc.) using Super Glue (a fast-curing cyanoacrylate formulation). The dialysis membrane that forms the "floor" of the observation volume had an 8000 Da MWCO. This specification, for globular proteins, corresponds to a pore diameter of about 13 Å. The dialysis membrane is pressed against the etched Teflon spacer and in turn against the cover glass and machined PTFE housing, using O-rings. The exchange fluid is circulated from a large beaker into the area underneath the dialysis membrane, fabricated from PTFE. The large dialysis area ($\sim$0.65 in.^{2}), together with the thinness of the sample, about 0.3 mm, facilitates rapid dialysis. The exchange fluid is typically circulated through the subchamber from a large beaker at a rate of about 3 mL/min.

After extensive dialysis against pure water, but without precautions to prevent dissolved CO_2, LNaPSS becomes difficult to photobleach. The pH of the dialysis fluid is then adjusted either with 0.4 mM phosphate buffer at pH 7 or 80 μM NaOH ($\sim$ pH 10). The adjustment of salt concentration was done by directly adding NaCl into the dialysis exchange fluid. Figure 5

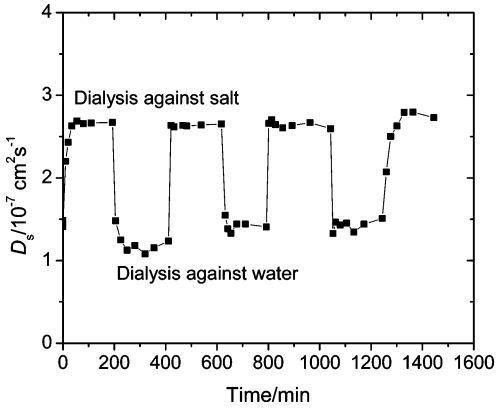

Figure 5. Reversibility of added salt on the apparent self-diffusion coefficient of fluoresceinamine labeled NaPSS-70K at 25 °C and 1.54 mg/mL.

shows the time response of the self-diffusion coefficient of LNaPSS-70K at 1.54 mg/mL upon the addition of NaCl. Soon after LNaPSS-70K was loaded into the dialysis cell, the self-diffusion coefficient was measured to be 1.46×10^{-7} cm^2 s^{-1}. The self-diffusion coefficient was monitored while the sample was being dialyzed against the bath fluid containing 25 mM NaCl. It increased to a steady-state value at 2.66×10^{-7} cm^2 s^{-1} in less than 1 h. The increased diffusion can be understood as a more compact chain moving faster; though relatively dilute, the chain also becomes even less aware of the presence of neighbors because these are similarly reduced in size. Incidentally, the increase in viscosity due to the added NaCl is very slight.[61] After dialysis against salt solution for ~3 h, the sample was dialyzed back against pure water that had been sonicated to remove CO_2 and adjusted with 80 μM NaOH. The self-diffusion coefficient fell to an average value of 1.17×10^{-7} cm^2 s^{-1}, significantly lower than the starting value. The original dialysis fluid containing NaCl was then reused, and the self-diffusion rose to a value of 2.64×10^{-7} cm^2 s^{-1}, identical within the experimental error (~2%) to that seen in the first salt cycle. This trend was continued for two more cycles. When the sample was subsequently dialyzed against water, the self-diffusion coefficient stabilized at 1.43×10^{-7} cm^2 s^{-1} for both cycles. The difference between the initial, low-salt value of 1.17×10^{-7} cm^2 s^{-1} and readings of 1.43×10^{-7} cm^2 s^{-1} on subsequent cycles is ascribed to pickup of CO_2 in the circulating dialysis fluid over time. The dialysis FPR cell performs well, giving a fast response to the added salt. The reversible time response indicates that the change in self-diffusion coefficient is solely due to the added salt.

The quantitative effect of NaCl on LNaPSS was further investigated with LNaPSS-167K at 1.5 mg/mL. Figure 6 shows the normalized contrast decays on a semilogarithmic K^2t scale. (The squared spatial frequency scaling is chosen because the optical settings were changed during the course of the experiments; it has been established that LNaPSS follows a K^2 dependence.[62]) The self-diffusion coefficient of LNaPSS-167K increases with the addition of NaCl, in a same manner mentioned above. At the lowest salt concentration, 0.08 mM, the value of self-diffusion coefficient reflects the extended coil conformation of labeled NaPSS, not any larger aggregate. In other words, no substantial long-range ordering of LNaPSS exists on the FPR experimental time scale.

Tanahatoe and Kuil calculated the diffusion coefficient for NaPSS-77K at infinite dilution (D_0) at various salt concentrations based on a wormlike chain model, including the persistence length, the excluded volume, and the counterion condensation.[63,64] Their results are shown in Figure 7, along with our dialysis FPR measurements of LNaPSS-167K. A linear relationship between the self-diffusion coefficient and logarithmic salt concentration is obtained at moderate values of salt.

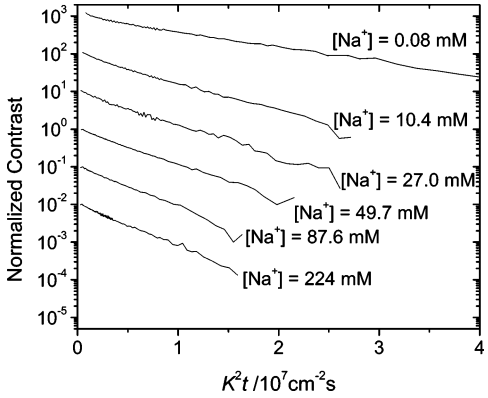

Figure 6. Effect of added salt on the FPR contrast decay of LNaPSS-167K at 25 °C. Concentration of LNaPSS-167K: 1.57 mg/mL. Traces have been offset vertically for clarity.

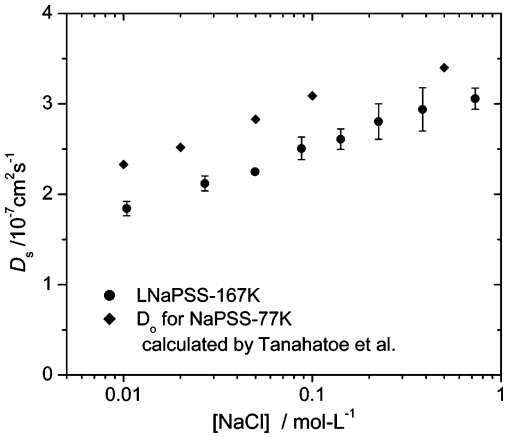

Figure 7. Effect of added salt on the optical tracer self-diffusion coefficient of LNaPSS-167K at 1.57 mg/mL and 25 °C (circles). Also shown are results from ref 63; see text.

Dobrynin, Rubinstein, and Colby[65] (DRC) made specific predictions for the variation of D_s with salt. Their eq 41 for dilute polyelectrolyte solutions predicts

$$D_s \approx (kT/\eta b)N^{-3/5}(cb^3)^{1/5}B^{2/5}(1 + 2Ac_s/c)^{1/5} \qquad (1)$$

where the new symbols are η = viscosity, b = monomer size, N = the number of monomers in the chain, $B = Nb/L$ where L is the contour length, and A = the number of monomers between uncondensed charges. DRC suggest $b = 3$ Å for NaPSS. Other parameters relevant to our experiment are $N = 811$ for LNaPSS-167K and 1 cP for the viscosity of water. In eq 1, concentrations are expressed as number density. The monomer mass of NaPSS is 206 g/mol, so 1.57 mg/mL, the concentration at which our measurements in Figure 7 were made, corresponds to 7.62 mM, i.e., 4.59×10^{18} cm^{-3}. In principle, the only remaining parameters, A and B, can be determined by fitting, but the results are very sensitive to choices for the denominator of eq 1. In place of a generic ηb, one might specify $3\pi\eta b$ for stick boundary conditions. In this case, an unweighted least-squares fit produced the smooth curve shown in Figure 8, corresponding to $A \approx 1.6$ and $B \approx 11$. When analyzing various experimental results, DRC more typically found $A \approx 5$ and $B \approx 3$. One possible explanation for the discrepancy could be the concentration at which our data were obtained. According to the very useful plot published by

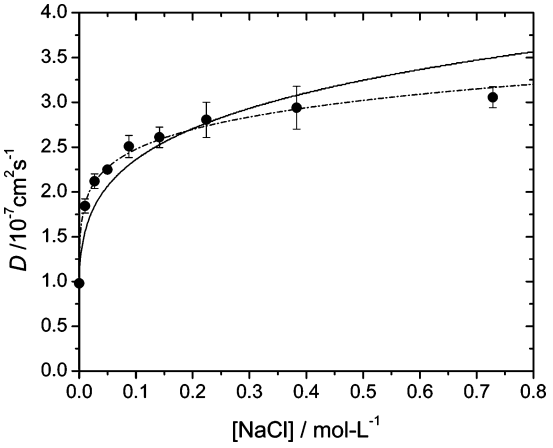

Figure 8. Comparison of LNaPSS-167K data from Figure 7 to theory of Dobrynin.[64] Solid curve: fit parameters A and B in eq 1. Dashed curve: fit $D_{c_s=0}$, K_s, and x in eq 2.

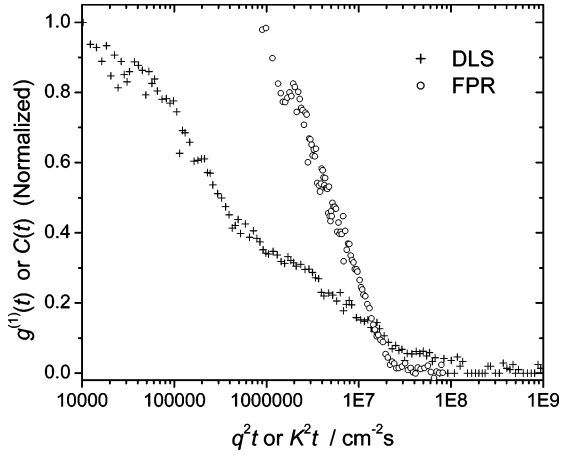

Figure 9. DLS and FPR signals for a mixed LNaPSS-70K/NaPSS-70K solution at 3 mM NaN_3, scaled for the different spatial frequencies of the two experiments. Total concentration of NaPSS: 30 mg/mL.

Boris and Colby (their Figure 4), the dialysis FPR experiments of Figures 7 and 8 were conducted beyond the overlap condition, but still far from the entangled limit. Another DRC equation (their eq 45) covers the semidilute, unentangled regime, but it was not successful in describing our data. Finally, Figure 8 shows that the dialysis FPR data were very well fit to an equation based on the form of eq 1. We write

$$D_s = D_{c_s=0}(1 + K_s c_s)^x \qquad (2)$$

where $D_{c_s=0}$, K_s, and x are adjustable parameters. Unfortunately, $D_{c_s=0}$ and K_s cannot be determined well by nonlinear least-squares analysis—many combinations suffice to fit the data—but the exponent is well determined: $x = 0.123 \pm 0.007$. The data of Tanahatoe and Kuil follow the form of eq 2 (but not quite as well; see plot in Supporting Information) with $x = 0.095 \pm 0.025$; again the parameters $D_{c_s=0}$ and K_s cannot be determined well.

For a monodisperse, dyed polymer, the ideal FPR trace is a straight line in the semilogarithmic representation chosen for Figure 6. All of the plots for NaPSS-167K demonstrate some curvature, suggesting polydispersity. Multiple factors may contribute to the slightly increased curvature at low ionic strength. One expects that β in the scaling relation $D \sim M^{-\beta}$ would rise as the ionic strength is reduced, reflecting the increased extension of the macromolecule in the absence of screening. Such "stretching" of the D vs M relation would render mass polydispersity more easily visible. Odijk and Houwaart[66] pointed out that the electrostatic persistence length depends on chain length; in a polydisperse sample, some molecules in the distribution stiffen more than others as salt is reduced. Finally, although there is no sharp biexponential behavior in Figure 6 to suggest a permanent population of slow diffusers, the enhanced curvature at low salt may reflect that a variable portion of diffusers are engaged in the putative temporal aggregates, perhaps for a varied amount of time. Experiments with rigid polyelectrolytes might eventually help to resolve some of these possibilities (thanks to a reviewer for this suggestion). Meanwhile, comparing the DLS and FPR characteristic times will provide valuable clues.

Comparison of DLS and FPR. Instead of the continuous, spontaneous coming and going of small concentration fluctuations that DLS monitors, FPR follows the evolution of a suddenly induced change in the local concentration of active fluorophores. The fluorescence profile of a solution is altered by 10% or less during typical photobleaching on our modulation FPR apparatus, but the polymer concentration profile is not perturbed at all. Assuming that a polymer molecule whose fluorophore has been "erased" has an almost identical chemical potential to one whose fluorophore is still intact, FPR should produce a close approximation to the self-diffusion coefficient. To compare the different behavior of DLS and FPR in experiments at low ionic strength, it is desirable to perform DLS and FPR on the exact same sample. To avoid self-quenching of the fluorescence at the relatively high concentrations convenient for DLS measurement with a weak HeNe laser that will not destroy the dye, a mixture of LNaPSS-70K and NaPSS-70K at 10:90 (w/w) was prepared. The total polymer concentration was 30 mg/mL, corresponding to $c_{DD} \approx 40$ mM. The same extensive cleaning procedure described for virgin NaPSS was used, except that 500 mM NaCl was chosen as the starting concentration and an extra filtration step (0.1 μm Millex VV) was inserted after exchange with 3 mM NaN_3. The latter alteration may slightly diminish the slow mode amplitude. Figure 9 overlays the DLS and FPR results in 3 mM NaN_3, adjusting for the large difference in the distance scale of the experiments, $2\pi/q = 621$ nm for DLS vs $2\pi/K = 107\,700$ nm for FPR. The DLS data are very noisy; it is difficult to measure low-salt solutions with the weak, red HeNe laser, but the stronger lines from the available argon ion or frequency-doubled diode lasers would destroy the dye (a krypton ion laser with powerful red line was unavailable). As with the above-described dialysis FPR studies on LNaPSS-70K, essentially one decay mode was observed (a weak, possibly spurious, fast decay process at very low salt requires further study). The DLS result clearly shows a biexponential character. The various decay rates and associated DLS amplitudes detected by FPR and DLS appear in Figure 10.

The error bars represent repeat CONTIN analyses with slightly different settings. The DLS slow modes at the two highest salt concentrations should probably be ignored, as they represent only 5% or 8% of signal and have large associated errors due to the noise in these correlation functions. Neglecting those two points, the behavior calls to mind Figure 3, which is based on quieter DLS data. Including the FPR results, the behavior is strongly reminiscent of that reported by Sehgal and Seery[67] for a commercial NaPSS and its labeled counterpart in a high-dielectric, nonaqueous solvent, *N*-methylformamide. In both studies, the self-diffusion values from FPR exceed those estimated from the DLS slow mode. This probably has to do with the lifetime of the structures responsible for the DLS slow

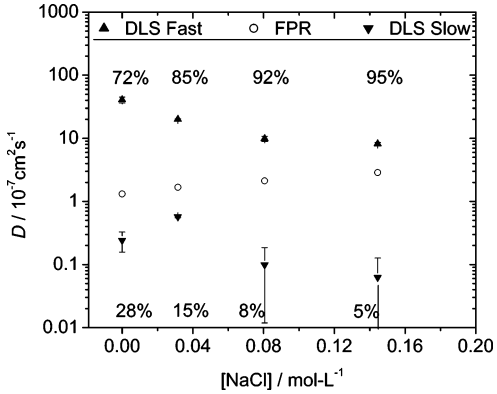

Figure 10. Combined DLS (fast, ▲; slow, ▼) and FPR (○) diffusion results as a function of added salt, using exactly the same samples for both techniques. For DLS, percent fast and slow scattering mode amplitudes are indicated.

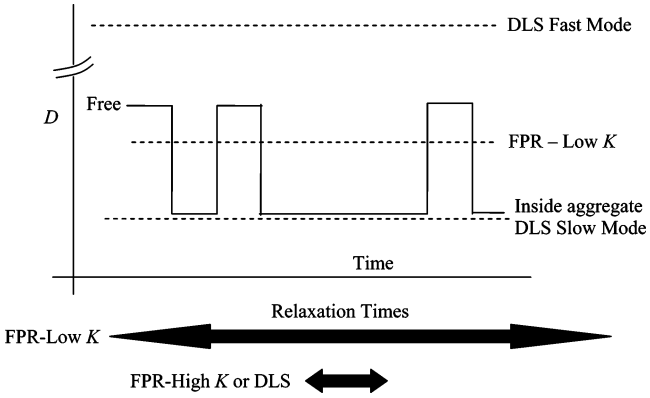

Figure 11. Proposed relation between DLS and FPR diffusion modes. The diffusion coefficient of a single chain changes as it enters and leaves temporal aggregates. Frequent interchange over the course of FPR measurements at low values of spatial frequency, K, results in a single-exponential recovery profile and a diffusion coefficient that is a weighted average of the free and in-aggregate values.

mode and the residence time of individual chains in the aggregate.

To register as a separate mode in DLS, a structure must maintain integrity long enough to diffuse a distance $X = 2\pi/q$. Taking 2.5×10^{-8} cm^2 s^{-1} as the DLS slow mode diffusion coefficient, and using the Einstein relation, $\langle X^2 \rangle = 2Dt$, between mean-squared displacement, diffusion coefficient, and time, a lifetime of at least 50 ms is required. While diffusing through a distance that is 240 times larger in our FPR experiments, a given polymer molecule may sample the temporal aggregates many times, spending the remainder of its time as a free diffuser. It would then register as a single diffuser with an average diffusion rate given by $D_{avg} = x_{free}D_{free} + (1 - x_{free})D_{aggregate}$, where x_{free} is the fraction of time spent away from the aggregate and D_{free} is the associated self-diffusion (and *not* the same as D_{fast} from DLS). Molecules must transfer to and from the aggregate rapidly on the ca. 20 s time scale of the FPR measurement. A lifetime of at least 0.05 s and a single chain residence time of <20 s are suggested.

Conclusion

Fully substituted NaPSS, never dried and without any provocation such as filtering, exhibits a reversible slow decay mode in DLS at low ionic strength in water. One merely needs to reduce the ionic strength by dialysis and reconcentrate the system by centrifugation of the dialysis DLS cell. The slow decay mode was observable even without reconcentrating the sample, so centrifugal force and associated hydrostatic pressure cannot be invoked as another source of the slow mode. This result supports other studies designed to minimize hydrophobic effects.[7,16,18,32] The multirun measurement protocol, low concentrations, and small detected volumes of our conventional DLS setup may be factors contributing to the generally small amplitudes of the slow modes detected here.

It is a safe bet that the FPR results in Figures 7 and 8 represent a lot less work than the DLS measurements of Tanahatoe and Kuil, also displayed. It is believed that these dialysis FPR studies well represent the self-diffusion behavior of unlabeled NaPSS because (1) fluoresceinamine-labeled NaPSS remains easily photobleachable as long as the pH is not too low, so heating during photobleaching is not likely an issue, (2) GPC/MALLS studies on fluorescein isothiocyanate-labeled NaPSS-*co*-allylamine suggested that labeling causes no serious alteration to chain conformation,[49] and (3) reversible expansion and contraction was so easily demonstrated (Figure 5). Additional testing of eqs 1 and 2 seems advisable, and with dialysis FPR it may come quickly.

When measuring the very same samples containing NaPSS and LNaPSS of the same molar mass, the optical tracer self-diffusion coefficient from FPR is sandwiched between the DLS slow and fast modes. Similar results were observed by Sehgal and Seery for NaPSS in *N*-methylformamide, although during their DLS measurement the labeled polymer was not present as it is (in minority composition) in ours. The FPR diffusion is not an average of the DLS modes, though. Until such time as a satisfactory molecular interpretation is devised, and in that regard simulations[68] may prove useful, the fast DLS mode is probably easiest to understand as the response of an osmotically stiff system to spontaneous fluctuations. The slow DLS mode may represent multimacroion domains that last long enough as integral bodies to dephase scattered light in DLS by traveling the small distance $2\pi/q$. Said domains are postulated to be loosely structured, such that the residence time of a single chain is shorter than the time required to travel the distance $2\pi/K$ to erase the imposed fluorophore contrast in FPR. In this scenario, schematically shown in Figure 11, the effectively single decay mode detected by FPR reflects a weighted average of the multimacroion diffusion coefficient and the self-diffusion coefficient of single chains that may enter and leave that aggregate during the much longer recovery time of FPR measurements. The hypothesis might be tested, and the residence time of chains in the temporal aggregates firmly established, using an FPR instrument that works on shorter distance scales (see, for example, ref 69). Obtaining high signal quality despite short recovery times may prove challenging for lightly labeled polymer. The modest, salt-dependent nonexponentiality observed in Figure 6 makes it impossible to rule out variation in how often the macromolecules exchange with the temporal aggregates. It is hoped that the simple dialysis extensions to DLS and FPR presented here will accelerate future polyelectrolyte studies targeting the remaining issues.

Acknowledgment. This work was supported by the National Science Foundation DMR-0075810 and DGE-9987603. The dialysis FPR cell was constructed under the auspices of the National Institute on Aging through Grant AG17983. We thank M. Muthukumar for insightful comments, and we equally thank the reviewers for helpful critiques and suggestions.

Supporting Information Available: Detailed description of the purification of the virgin NaPSS solutions, determination of the UV extinction coefficient for sodium poly(styrenesulfonate), sample

preparation procedures for DLS, measurement details for DLS, isolation of a high-*M* fraction of LNaPSS, analysis of the data of ref 63 using eq 2, and DLS line-shape analysis. This material is available free of charge via the Internet at http://pubs.acs.org.

References and Notes

(1) Lin, S.-C.; Lee, W. I.; Schurr, J. M. *Biopolymers* **1978**, *17*, 1041−1064.
(2) Lee, W. I.; Schurr, J. M. *J. Polym. Sci., Polym. Phys. Ed.* **1975**, *13*, 873−888.
(3) Zimm, B. H.; Stein, R. S.; Doty, P. *Polym. Bull. (Berlin)* **1945**, *1*, 90−119.
(4) Yamakawa, H. *Modern Theory of Polymer Solutions;* Harper and Row: New York, 1971.
(5) Ghosh, S.; Li, X.; Reed, C. E.; Reed, W. F. *Biopolymers* **1990**, *30*, 1102−1112.
(6) Drifford, M.; Dalbiez, J.-P. *Biopolymers* **1985**, *24*, 1501−1514.
(7) Topp, A.; Belkoura, L.; Woermann, D. *Macromolecules* **1996**, *29*, 5392−5397.
(8) Sedlak, M. *Langmuir* **1999**, *15*, 4045−4051.
(9) Schmitz, K. S.; Lu, M.; Singh, N.; Ramsay, D. J. *Biopolymers* **1984**, *23*, 1637−1646.
(10) Schmitz, K. S.; Ramsay, D. J. *Biopolymers* **1985**, *24*, 1247−1256.
(11) Zero, K.; Ware, B. R. *J. Chem. Phys.* **1984**, *80*, 1610−1616.
(12) Schmitz, K. S. An Overview of Polyelectrolytes. In *Macro-ion Characterization From Dilute Solutions to Complex Fluids*; ACS Symposium Series No. 548; Schmitz, K. S., Ed.; American Chemical Society: Washington, DC, 1994; Chapter 1, pp 1−22.
(13) Schmitz, K. S. *Macro-ion Characterization from Dilute Solutions to Complex Fluids;* American Chemical Society: Washington, DC, 1994; Vol. 548.
(14) Sedlak, M.; Amis, E. J. *J. Chem. Phys.* **1992**, *96*, 817−825.
(15) Matsuoka, H.; Schwahn, D.; Ise, N. *Macromolecules* **1991**, *24*, 4227−4228.
(16) Ermi, B. D.; Amis, E. J. *Macromolecules* **1998**, *31*, 7378−7385.
(17) Prabhu, V. M.; Amis, E. J.; Bossev, D. P.; Rosov, N. *J. Chem. Phys.* **2004**, *121*, 4424−4429.
(18) Sehgal, A.; Seery, T. A. P. *Macromolecules* **1998**, *31*, 7340−7346.
(19) Amis, E. J.; Valachovic, D. E.; Sedlak, M. Structure and Dynamics of Linear Flexible Polyelectrolytes in Salt-free Solution as Seen by Light Scattering. In *Macro-ion Characterization From Dilute Solutions to Complex Fluids*; ACS Symposium Series No. 548; Schmitz, K. S., Ed.; American Chemical Society: Washington, DC, 1994; Chapter 25, pp 322−336.
(20) Ghosh, S.; Peitzsch, R. M.; Reed, W. F. *Biopolymers* **1992**, *32*, 1105−1122.
(21) Michel, R. C.; Reed, W. F. *Biopolymers* **2000**, *53*, 19−39.
(22) Reed, W. F.; Ghosh, S.; Medjahdi, G.; Francois, J. *Macromolecules* **1991**, *24*, 6189−6198.
(23) Reed, W. F. *Macromolecules* **1994**, *27*, 873−874.
(24) Reed, W. F. Light Scattering Results on Polyelectrolyte Conformations, Diffusion, and Interparticle Interactions and Correlations. In *Macro-ion Characterization From Dilute Solutions to Complex Fluids*; ACS Symposium Series No. 548; Schmitz, K. S., Ed.; American Chemical Society: Washington, DC, 1994; Chapter 23, pp 297−314.
(25) Sedlak, M.; Amis, E. J. *J. Chem. Phys.* **1992**, *96*, 826−834.
(26) Sedlak, M. *J. Chem. Phys.* **1997**, *107*, 10799−10804.
(27) Sedlak, M. Extraordinary Behavior of Salt-free Solutions of Strongly Charged Polyelectrolytes. In *Macro-ion Characterization From Dilute Solutions to Complex Fluids*; ACS Symposium Series No. 548; Schmitz, K. S., Ed.; American Chemical Society: Washington, DC, 1994; Chapter 26, pp 337−348.
(28) Sedlak, M. *J. Chem. Phys.* **2002**, *116*, 5256−5262.
(29) Sedlak, M. *J. Chem. Phys.* **2002**, *116*, 5246−5255.
(30) Sedlak, M. *J. Chem. Phys.* **2002**, *116*, 5236−5245.
(31) Sedlak, M. *J. Chem. Phys.* **1996**, *105*, 10123−10133.
(32) Ermi, B. D.; Amis, E. J. *ACS Polym. Prepr.* **1995**, *36*, 371−372.
(33) Sohn, D.; Russo, P. S.; Roitman, D. B. *Ber. Bunsen-Ges. Phys. Chem.* **1996**, *100*, 821−828.
(34) Yu, K.; Russo, P. S. *J. Polym. Sci., Polym. Phys. Ed.* **1996**, *34*, 1467−1475.
(35) Matsuoka, H.; Ogura, Y.; Yamaoka, H. *J. Chem. Phys.* **1999**, *109*, 6125−6132.
(36) Brown, D. W.; Lowry, R. E. *J. Polym. Sci., Part A*: *Polym. Chem.* **1979**, *17*, 1039−1046.
(37) Baigl, D.; Seery, T. A. P.; Williams, C. E. *Macromolecules* **2002**, *35*, 2318−2326.
(38) Sedlak, M. *J. Chem. Phys.* **1994**, *101*, 10140−10144.
(39) Valachovic, D. E.; Amis, E. J.; Tomalia, D. A. *ACS Polym. Prepr.* **1995**, *36*, 373−374.
(40) Smits, R. G.; Kuil, M. E.; Mandel, M. *Macromolecules* **1994**, *27*, 5599−5608.
(41) Porsch, B.; Sundelof, L.-O. *Macromolecules* **1995**, *28*, 7165−7170.
(42) Phillies, G. D. J.; O'Connell, R.; Whitford, P.; Streletzky, K. A. *J. Chem. Phys.* **2003**, *119*, 9903−9913.
(43) Stepanek, P.; Brown, W.; Hvidt, S. *Macromolecules* **1996**, *29*, 8888−8893.
(44) Wang, C. H. *J. Chem. Phys.* **1991**, *95*, 3788.
(45) Brown, W.; Stepanek, P. *Macromolecules* **1993**, *26*, 6884−6890.
(46) Wang, L.; Garner, M. M.; Yu, H. *Macromolecules* **1991**, *24*, 2368−2376.
(47) Yoon, H.; Kim, H.; Yu, H. *Macromolecules* **1989**, *22*, 848.
(48) Sohn, D.; Russo, P. S.; Davila, A.; Poche', D. S.; McLaughlin, M. L. *J. Colloid Interface Sci.* **1996**, *177*, 31−44.
(49) Cong, R.; Turksen, S.; Russo, P. S. *Macromolcules* **2004**, *37*, 4731−4735.
(50) Prabhu, V. M.; Muthukumar, M.; Wignall, G. D.; Melnichenko, Y. B. *Polymer* **2001**, *42*, 8935−8946.
(51) Borochov, N.; Eisenberg, H. *Macromolecules* **1994**, *27*, 1440−1445.
(52) Sehgal, A. Ph.D. Thesis, University of Connecticut, 2000.
(53) Koppel, D. E. *J. Chem. Phys.* **1972**, *57*, 4814−4820.
(54) Mustafa, M. B.; Tipton, D. L.; Barkley, M. D.; Russo, P. S.; Blum, F. D. *Macromolecules* **1993**, *26*, 370−378.
(55) Fong, B.; Stryjewski, W.; Russo, P. S. *J. Colloid Interface Sci.* **2001**, *239*, 374−379.
(56) Berne, B.; Pecora, R. *Dynamic Light Scattering*; Wiley: New York, 1976.
(57) Kaye, W.; McDaniel, J. B. *Appl. Opt.* **1974**, *13*, 1934−1937.
(58) Provencher, S. W. *Comput. Phys.* **1982**, *27*, 213−227.
(59) Provencher, S. W. *Comput. Phys.* **1982**, *27*, 229−242.
(60) Oostwal, M.; Odijk, T. *Macromolecules* **1993**, *26*, 6489−6497.
(61) Mazurkiewicz, J.; Tomasik, P.; Zaplotny, J. *Food Hydrocolloids* **2001**, *15*, 43−46.
(62) Jamil, T.; Russo, P. S. *Langmuir* **1998**, *16*, 266−270.
(63) Tanahatoe, J. J.; Kuil, M. E. *Macromolecules* **1997**, *30*, 6102−6106.
(64) Tanahatoe, J. J.; Kuil, M. E. *J. Phys. Chem. A* **1997**, *101*, 8389−8394.
(65) Dobrynin, A. V.; Colby, R. H.; Rubinstein, M. *Macromolecules* **1995**, *28*, 1859−1871.
(66) Odijk, T.; Houwaart, A. C. *J. Polym. Sci., Polym. Phys. Ed.* **1978**, *16*, 627−639.
(67) Sehgal, A.; Seery, T. A. P. *Macromolecules* **2003**, *36*, 10056−10062.
(68) Chang, R. W.; Yethiraj, A. *J. Chem. Phys.* **2002**, *116*, 5284−5298.
(69) Cicerone, M. T.; Blackburn, F. R.; Ediger, M. D. *Macromolecules* **1995**, *28*, 8225−8232.

MA051171X